

ULTRAVIOLET OBSERVATIONS OF SUPER-CHANDRASEKHAR MASS TYPE Ia SUPERNOVA CANDIDATES WITH SWIFT UVOT

PETER J. BROWN¹, PAUL KUIN², RICHARD SCALZO³, MICHAEL SMITKA¹,
MASSIMILIANO DE PASQUALE², STEPHEN HOLLAND⁴, KEVIN KRISCIUNAS¹,
PETER MILNE⁵, LIFAN WANG¹

Draft version October 17, 2018

ABSTRACT

Among Type Ia supernovae (SNe Ia) exist a class of overluminous objects whose ejecta mass is inferred to be larger than the canonical Chandrasekhar mass. We present and discuss the UV/optical photometric light curves, colors, absolute magnitudes, and spectra of three candidate Super-Chandrasekhar mass SNe—2009dc, 2011aa, and 2012dn—observed with the *Swift* Ultraviolet/Optical Telescope. The light curves are at the broad end for SNe Ia, with the light curves of SN 2011aa being amongst the broadest ever observed. We find all three to have very blue colors which may provide a means of excluding these overluminous SNe from cosmological analysis, though there is some overlap with the bluest of “normal” SNe Ia. All three are overluminous in their UV absolute magnitudes compared to normal and broad SNe Ia, but SNe 2011aa and 2012dn are not optically overluminous compared to normal SNe Ia. The integrated luminosity curves of SNe 2011aa and 2012dn in the UVOT range (1600–6000 Å) are only half as bright as SN 2009dc, implying a smaller ⁵⁶Ni yield. While not enough to strongly affect the bolometric flux, the early time mid-UV flux makes a significant contribution at early times. The strong spectral features in the mid-UV spectra of SNe 2009dc and 2012dn suggest a higher temperature and lower opacity to be the cause of the UV excess rather than a hot, smooth blackbody from shock interaction. Further work is needed to determine the ejecta and ⁵⁶Ni masses of SNe 2011aa and 2012dn and fully explain their high UV luminosities.

Subject headings: supernovae: general — supernovae: individual (SN2009dc, SN2011aa, SN2012dn)
— ultraviolet: general

1. CANDIDATE SUPER-CHANDRASEKHAR MASS TYPE Ia SUPERNOVAE

Type Ia Supernovae (SNe Ia) are important cosmological probes that first revealed the accelerating expansion of the universe (Riess et al. 1998; Perlmutter et al. 1999). The cosmological results rely on the normal SNe Ia whose brightness correlates with their light curve shapes and colors (Phillips et al. 1999; Riess et al. 1996; Goldhaber et al. 2001), allowing them to be used as standardizable candles. Observations of similar but peculiar objects are useful for understanding the nature of the progenitor systems and the physics of the explosion, particularly how they might differ between objects. It is also important to understand objects which may be found in cosmological samples but do not follow the relationships between the luminosity and the light curve shape.

The similar peak luminosities of SNe Ia suggested explosions of similar mass and energy. The widely-held theory is that a SN Ia results from the thermonuclear disruption of a Carbon-Oxygen white dwarf (CO-WD) as it ap-

proaches the Chandrasekhar limit. This could be due to accretion from a non-degenerate companion (also called the single degenerate scenario; Whelan & Iben 1973) or the disruption of a WD companion (also called the double degenerate scenario; Webbink 1984; Iben & Tutukov 1984). The nature of an SN Ia progenitor as a C-O WD (and admittedly for a single case) has only recently been confirmed by very early time observations of SN 2011fe (Nugent et al. 2011; Bloom et al. 2012). The WD mass at explosion might not need approach the Chandrasekhar limit, as helium shell detonations can trigger a core detonation in sub-Chandrasekhar mass progenitors (Woosley & Weaver 1994; Fink et al. 2010; Kromer et al. 2010; Woosley & Kasen 2011).

The nature of the companion remains unknown, and recent results suggest that SNe Ia may result from both single degenerate and double degenerate systems. Early observations of many SNe Ia do not show the interaction expected (Kasen 2010) if the SN explosion were to interact with a red giant (RG) companion (Hayden et al. 2010; Bianco et al. 2011; Ganeshalingam et al. 2011; Brown et al. 2012a). X-ray limits also rule out red giants due to the lack of shock interaction (Russell & Immler 2012). Pre-explosion, multi-wavelength, and extremely early observations of SN 2011fe rule out a RG (Nugent et al. 2011; Li et al. 2011; Horesh et al. 2012; Margutti et al. 2012) and even a main sequence (MS) companion (Bloom et al. 2012; Brown et al. 2012b) for that object. Searches for the leftover companion in SNR 0509-67.5 rule out a non-degenerate companion (Schaefer & Pagnotta 2012). On

¹ George P. and Cynthia Woods Mitchell Institute for Fundamental Physics & Astronomy, Texas A. & M. University, Department of Physics and Astronomy, 4242 TAMU, College Station, TX 77843, USA; pbrown@physics.tamu.edu

² Mullard Space Science Laboratory, University College London, Holmbury St. Mary, Dorking Surrey, RH5 6NT, UK

³ Research School of Astronomy and Astrophysics, The Australian National University, Mount Stromlo Observatory, Cotter Road, Weston Creek ACT 2611, Australia

⁴ Space Telescope Science Center 3700 San Martin Dr., Baltimore, MD 21218, USA

⁵ Steward Observatory, University of Arizona, Tucson, AZ 85719, USA

the other hand, high resolution spectroscopy of nearby SNe has found a preference for blue shifted sodium absorption in about 20-25% of SNe Ia (Sternberg et al. 2011; Foley et al. 2012a; Maguire et al. 2013) and even variable absorption (Patat et al. 2007; Simon et al. 2009) suggestive of a local CSM wind from a non-degenerate companion. PTF11kx observations showed signatures of a recurrent nova progenitor in a single degenerate system (Dilday et al. 2012). Thus, multiple channels might be required to create the explosions classified as SNe Ia.

The idea that the accreting progenitor explodes as it approaches the Chandrasekhar mass has been challenged by a class of SNe that appear spectroscopically similar to SNe Ia but are overluminous for their light curve shape. Detailed modeling of the light curves appears to require more than a Chandrasekhar mass of ejected material. SN 2003fg was the first discovered (Howell et al. 2006) with SNe 2006gz (Hicken et al. 2007), 2007if (Scalzo et al. 2010; Yuan et al. 2010) and 2009dc (Yamanaka et al. 2009; Tanaka et al. 2010; Silverman et al. 2011; Taubenberger et al. 2011; Kamiya et al. 2012; Hachinger et al. 2012) showing similarities. Scalzo et al. (2012) discovered five additional, similar objects in SN Factory observations, though only one was conclusively above the Chandrasekhar limit. Association with this subclass is sometimes based on spectroscopic similarity to others of the class, to a high inferred luminosity, or to actually modeling the light curve and determining a high ejecta mass. Variations exist amongst candidates of this subclass, which is not surprising given our limited understanding of their origin and relationship to normal SNe Ia. Maeda & Iwamoto (2009) highlight the observational differences between SNe 2003fg and 2006gz, two probable super-Chandrasekhar mass candidates.

The most common means of estimating the mass from SNe Ia comes from the application of ‘‘Arnett’s Law’’ (Arnett 1982; Branch 1992). At maximum light the luminosity output is approximately equal to the instantaneous rate of energy release from radioactive decay. Thus the peak bolometric luminosity is proportional to the mass of ^{56}Ni synthesized in the explosion. The ^{56}Ni can also be estimated from the late light curve (Silverman et al. 2011) or nebular spectra (Mazzali et al. 1997). The total mass can be estimated based on energetics using the observed luminosities and expansion velocities and assumptions on the density profile (e.g. Scalzo et al. 2012). The mass can also be estimated by constructing models of various masses and explosion scenarios and comparing to the observed light curves (Kamiya et al. 2012) and spectra (Mazzali et al. 1997; Hachinger et al. 2012).

Not all of the luminosity necessarily comes from radioactive decay. Excess luminosity could also come from circumstellar interaction (Taubenberger et al. 2013) or result from asymmetric explosions viewed at a favorable angle (Hillebrandt et al. 2007). Asymmetric explosions cannot explain the brightest of SC SNe, and spectropolarimetry of SN 2009dc implies no large scale asymmetries in the plane of the sky (Tanaka et al. 2010). Maeda et al. (2009) find that the late time observations of SN 2006gz require less radioactive Ni than suggested from peak optical observations, drawing into question the overluminous nature of the event. They suggest that the

luminosity is overestimated due to an over-correction for extinction.

SC SNe are hot, high-energy explosions, so ultraviolet (UV) coverage is important to better measure the total luminosity and determine its origin, in particular whether it originates from shocks or simply a hot photosphere. The Ultraviolet/Optical Telescope (UVOT; Roming et al. 2005) on the Swift satellite (Gehrels et al. 2004) presents an excellent opportunity to obtain unique, early-time UV data. This paper will focus on three objects: SN 2009dc—a well-studied member of the Super-Chandrasekhar mass SN class—and SNe 2011aa and 2012dn which share some characteristics. We will refer to these candidate super-Chandrasekhar SNe Ia as SC SNe below, though a firm mass determination will require more data and is beyond the scope of this work. Comparisons will focus on the differences and similarities between SN 2009dc and the less studied SNe 2011aa and 2012dn, and the differences of these three SC SNe compared to other SNe Ia. In Section 2 we discuss these three SC SNe and present UV/optical photometry and spectra from UVOT. In Section 3 we compare the colors, absolute magnitudes, spectra, and integrated luminosities, comparing SNe 2011aa and 2012dn to 2009dc and the three to a larger sample of ‘‘normal’’ SNe Ia. In Section 4 we discuss the results and summarize.

2. SWIFT OBSERVATIONS OF CANDIDATE SUPER-CHANDRASEKHAR MASS SNe

2.1. SN2009dc

SN 2009dc was discovered by Puckett et al. (2009) on 2009 April 9.31 (all dates UT). Marion et al. (2009) reported spectroscopic similarities to SC SNe on April 22. Swift observations began April 25.5. Swift/UVOT photometry has been published by Silverman et al. (2011) and also referred to by Taubenberger et al. (2011). An epoch of UV grism spectroscopy was performed May 1.0 (4.9 days after the time of maximum light in the B-band). SN 2009dc has been extensively studied (Yamanaka et al. 2009; Tanaka et al. 2010; Silverman et al. 2011; Taubenberger et al. 2011) including theoretical modeling of the light curves (Kamiya et al. 2012) and spectra (Hachinger et al. 2012). Assuming that its luminosity is powered by radioactive decay, SN 2009dc likely had a ^{56}Ni yield between 1.2 and 1.8 M_{\odot} depending on the assumed extinction (though Silverman et al. 2011 also calculate a ^{56}Ni mass of 3.7 M_{\odot} for their largest plausible reddening).

SN 2009dc exploded outside of UGC 10064 toward the disrupted companion UGC 10063 (see Taubenberger et al. 2011 and Khan et al. 2011 for further discussion of the host environment). The redshift of UGC 10064 is 0.021391 ± 0.000070 (Falco et al. 1999). The foreground galactic extinction along the line of sight is $A_V=0.191$ (Schlafly & Finkbeiner 2011).

2.2. SN2011aa

SN 2011aa was discovered by Puckett et al. (2011) on 2011 February 6.3. It was also independently discovered by MASTER on 2011 February 13.54 (Kudolina et al. 2011). From optical spectra taken February 8.9 it was spectroscopically identified as a young SN Ia by Gurugubelli et al. (2011) who found a best match to the

normal SN Ia 1998aq a week before maximum light. Observations with the Swift spacecraft began on Feb 11.6 and continued for 16 epochs of UV and optical photometry (every other day around maximum light and then more spread out at later times). One epoch of spectroscopy with the UVOT's UV grism was performed on February 28.0 (8.1 days after maximum light in the B-band), but overlap with a field star significantly contaminates the spectrum. Kamiya (2012) found photometric similarities between SN 2011aa optical observations and SC SNe Ia models.

SN 2011aa is located at the intersection of two galaxies designated UGC3906 at a redshift of 0.012355 ± 0.000087 (de Vaucouleurs et al. 1991). The foreground galactic extinction along the line of sight is $A_V=0.078$ (Schlafly & Finkbeiner 2011).

2.3. SN2012dn

SN 2012dn was discovered by Bock et al. (2012) on 2012 July 8.5. Parrent & Howell (2012) spectroscopically classified it as a SN Ia before maximum light from a spectrum obtained July 10.2. They noted strong CII absorption and similarities to three SNe Ia described as SC SNe Ia. Copin et al. (2012) also noticed similarities to SC SNe Ia spectra. Swift observations began July 13.1. One epoch of UV grism spectroscopy was obtained on July 22.6 (2.2 days before maximum light in the B band). We also use an optical spectrum obtained by the South African Large Telescope (SALT) on July 24 from Parrent et al. (2013, in prep). The UVOT and SALT spectra were combined by normalizing to the same B-band magnitude and splicing together at 4750 \AA .

SN 2012dn is located in the galaxy ESO 462-G016 at a redshift of 0.010187 ± 0.000020 (Theureau et al. 1998). The foreground galactic extinction along the line of sight is $A_V=0.167$ (Schlafly & Finkbeiner 2011).

2.4. Data Reduction

The Swift/UVOT observations used the following six broadband filters with the corresponding central wavelengths (Poole et al. 2008): uvw2 (1928 Å), uvm2 (2246 Å), uvw1 (2600 Å), u (3465 Å), b (4392 Å), and v (5468 Å). Those filters are sometimes referred to as w2, m2, w1, uu, bb, and vv, respectively. Swift/UVOT data were analyzed following the methods of Poole et al. (2008) and Brown et al. (2009) but incorporating the revised UV zeropoints and time-dependent sensitivity from Breeveld et al. (2011). The photometry is given in Table 1. The light curves of the three SC SNe are displayed in Figure 1. The UVOT data for SN 2009dc were originally published in Silverman et al. (2011) and here we rereduce the data with the new zeropoints, sensitivity corrections, and subtraction of the underlying galaxy flux. The difference is small – typically less than 0.05 mag. The photometry for SN 2011aa also includes galaxy subtraction, so the late time flattening in the UV filters appears to be real. SN 2012dn does not have galaxy template images, but the amount of galaxy contamination is likely small. The UVOT b and v bands are similar to Johnson *B* and *V* while the Swift u-band is extends to much shorter wavelengths than Johnson *U* or Sloan *u'* (and does not suffer from atmospheric attenuation), of particular importance for SNe such as these with different

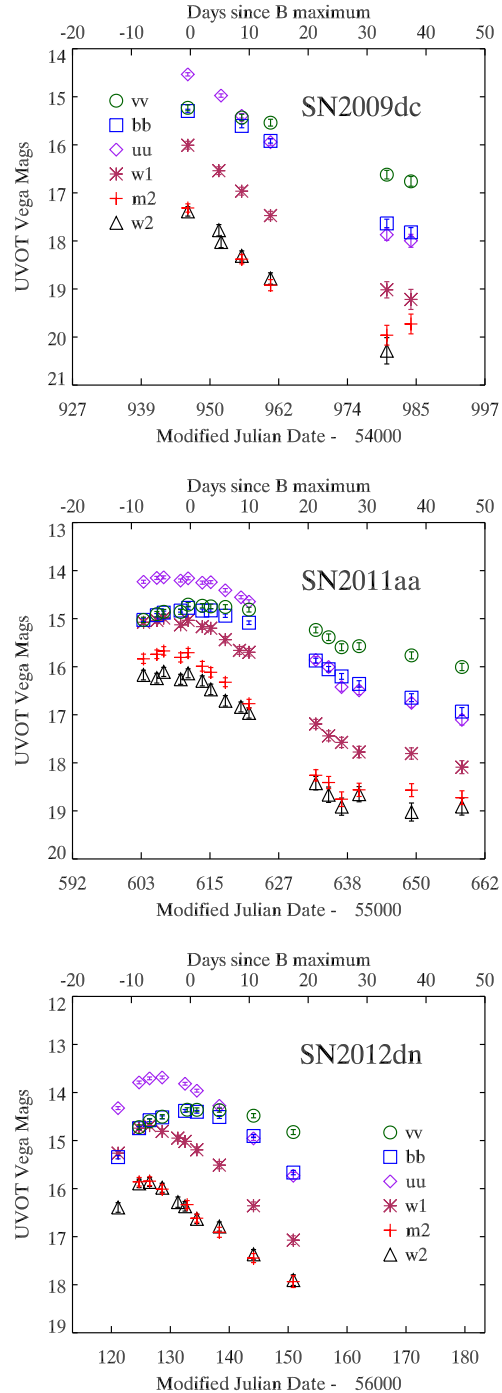


Figure 1. UVOT light curves of SNe 2009dc, 2011aa, and 2012dn. The same axis ranges are used for all SNe for a fair comparison.

UV spectral shapes than normal SNe. While we have obtained photometry in six bands, for simplicity we will focus on three filters with which to measure colors and absolute magnitudes. We use uvm2 for the mid-UV (or MUV), uvw1 for the near-UV (or NUV), and the v-band for the optical.

The UVOT grism data was extracted and calibrated using the default parameters of the UVOTPY package (Kuin et al. 2014, in preparation). The nominal wave-

⁶ www.mssl.ucl.ac.uk/www_astro/uvot

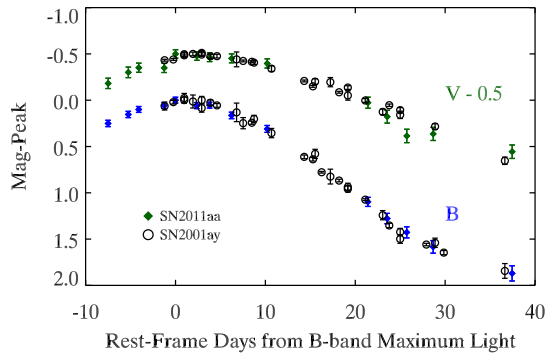


Figure 2. The b and v light curves of SN 2011aa compared to ground-based B and V of SN 2001ay from Krisciunas et al. (2011). The curves are shifted along the x-axis to the time of maximum light in the B band. The curves are shifted vertically to the peak-magnitude in the respective filter, with the v curves shifted by an additional 0.5 mag for clarity. The light curves of SN 2011aa are nearly identical to those of “the most slowly declining type Ia supernova” (Krisciunas et al. 2011).

length accuracy is 20 \AA and the flux calibration is accurate to about 10%. Individual exposures were extracted and the spectra combined using a weighted mean.

2.5. Comparison Type Ia Supernovae

For comparison, we use previously published photometry (updated to the latest calibration as described above) from spectroscopically normal SNe Ia with $\Delta m_{15}(B) < 1.4$ with detections in all three UV filters (Brown et al. 2010, 2012a). For SN 2011fe we use spectrophotometry of SN 2011fe using the spectra from Pereira et al. (2013) due to the UVOT data’s optical saturation near peak (Brown et al. 2012b). Further comparisons are made with SNe spectroscopically similar to SN 2002cx (SNe 2005hk and 2012Z) and SN 1991T (SNe 2007S, 2007cq, and 2011dn). The photometry from 2011dn is presented here for the first time while SN 2012Z will be presented in Stritzinger et al. (2014, in preparation) and the others were previously published in Brown et al. (2009).

3. RESULTS

3.1. Light Curves

The light curves of SNe 2009dc, 2011aa and 2012dn are shown in Figure 1. Swift observations of SN 2009dc began near maximum light so the curves monotonically fade, but all appear qualitatively very similar, including the crossing points of the different filters. The evolution of SN 2011aa, though, is much slower. We show in Figure 2 that it has a similar decay rate in b and v as SN 2001ay, “the most slowly declining type Ia supernova” (Krisciunas et al. 2011). The UV light curves are also broader than those of normal SNe Ia, most of which have very similar post-maximum light curve shapes in the NUV (Immler et al. 2006; Milne et al. 2010). We parameterize the light curves of SNe 2011aa and 2012dn by their peak magnitudes and by Δm_{15} , the number of magnitudes they fade in the 15 days following maximum light in that same band. The peak is determined by stretching a template light curve to the data between 5 days before and 5 days after maximum light. Δm_{15} is determined by stretching a template light curve to the data between 2 days before and 15 days after maximum

Table 1
UVOT Photometry

SN	Filter	MJD	Mag	M_Err	Rate	R_Err
SN2012dn	UVW2	56121.1333	16.393	0.100	2.482	0.230
SN2012dn	UVM2	56124.7118	15.857	0.089	2.495	0.204
SN2012dn	UVW1	56121.1419	15.262	0.056	7.434	0.383
SN2012dn	U	56121.1303	14.324	0.031	40.397	1.152
SN2012dn	B	56121.1313	15.344	0.036	32.096	1.059
SN2012dn	V	56124.7077	14.720	0.048	18.529	0.822

Note. — The full table is available in the electronic version. The photometry will also be available from the Swift SN website http://people.physics.tamu.edu/pbrown/SwiftSN/swift_sn.html.

Table 2
Light Curve Parameters

Parameters	SN2011aa	SN2012dn
$m_{w2}(\text{peak})$	16.15 ± 0.04	15.86 ± 0.04
$\Delta m_{15}(w2)$	0.97 ± 0.10	1.03 ± 0.06
$t_{max}(w2)-t_{max}(b)$	-4.4 ± 1.4	-7.1 ± 0.5
$m_{m2}(\text{peak})$	15.70 ± 0.04	15.84 ± 0.15
$\Delta m_{15}(m2)$	1.15 ± 0.08	1.02 ± 0.05
$t_{max}(m2)-t_{max}(b)$	-3.7 ± 1.2	-7.3 ± 1.6
$m_{w1}(\text{peak})$	15.01 ± 0.02	14.71 ± 0.02
$\Delta m_{15}(w1)$	0.78 ± 0.06	1.21 ± 0.05
$t_{max}(w1)-t_{max}(b)$	-4.9 ± 0.8	-7.0 ± 0.4
$m_u(\text{peak})$	14.14 ± 0.01	13.69 ± 0.01
$\Delta m_{15}(u)$	0.67 ± 0.02	1.14 ± 0.03
$t_{max}(u)-t_{max}(b)$	-4.3 ± 0.5	-5.0 ± 0.3
$m_b(\text{peak})$	14.80 ± 0.01	14.38 ± 0.07
$\Delta m_{15}(b)$	0.59 ± 0.07	1.08 ± 0.03
$m_v(\text{peak})$	14.73 ± 0.02	14.36 ± 0.10
$\Delta m_{15}(v)$	0.30 ± 0.07	0.44 ± 0.04
$t_{max}(v)-t_{max}(b)$	2.4 ± 0.7	0.6 ± 1.8

light to the data and interpolating from the stretched template. The UV templates (with uvw1 template also being used for u band due to its similar light curve shape) come from SN 2011fe (Brown et al. 2012b) and B and V from MLC2k2 (Jha et al. 2007). We note that for very broad SNe such as some of these, the measurement of light curve parameters depend heavily on how the fitting and determination of the peak time is done. The light curve parameters are tabulated in Table 2. We also list the difference in time between when the SN peaks in the b band compared to the other filters. The difference in peak times between b and uvw1 are much larger than the normal SNe analyzed by Milne et al. (2010) with a mean of 2.22 days and the largest being 3.7. SN 2009dc is excluded since observations began near the optical peak, while the UV was already fading.

The b-band light curves are found to peak at MJD 54947.1 (2009 April 26.1), 55611.9 (2011 February 19.9), and 56132.8 (2012 July 24.8) for SNe 2009dc, 2011aa, and 2012dn, respectively. These values are used as the reference epochs for the light curves and spectra displayed.

3.2. Colors

Figure 3 shows the color evolution in uvm2-uvw1 and uvw1-v of the three SC SNe Ia compared to spectroscopically normal Swift SNe with $\Delta m_{15}(B) < 1.4$. The left panel shows that the uvw1-v colors of normal SNe evolve from red to blue, reaching a minimum color a few days

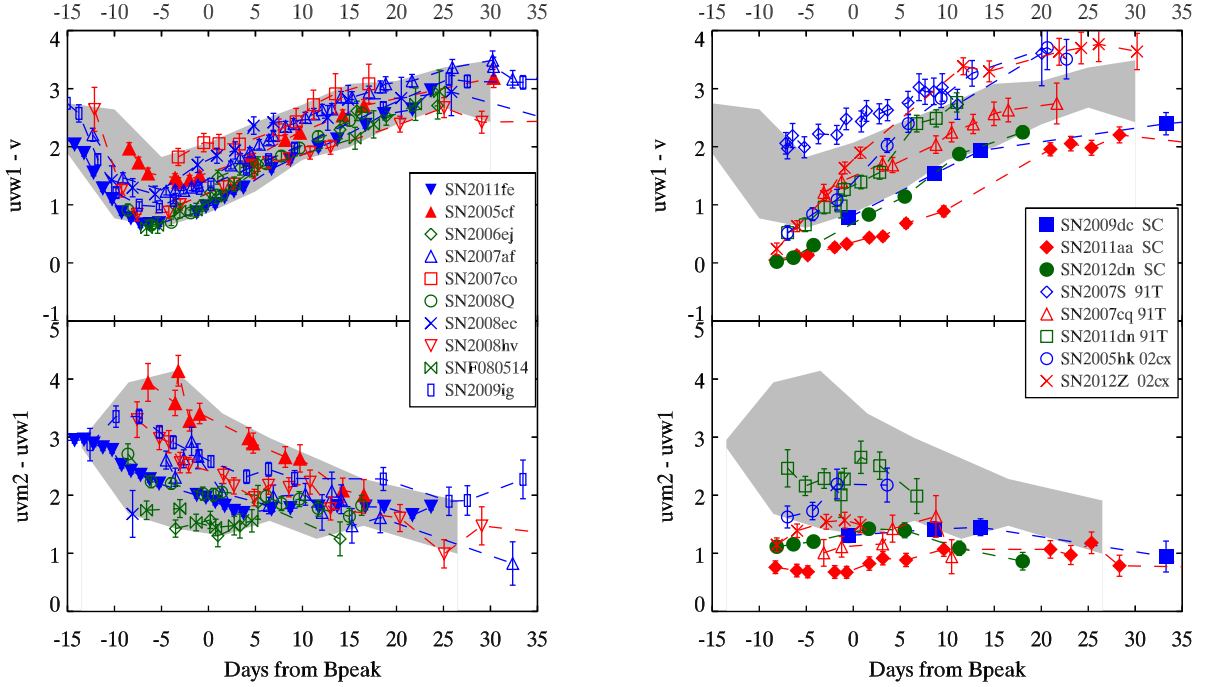


Figure 3. Left: $uvw1-v$ and $uvm2-uvw1$ colors of normal SNe Ia observed by Swift with shaded region showing their range of colors. The identification of individual color curves is not as important as the range of colors exhibited by “normal” SNe Ia. Right: $uvw1-v$ and $uvm2-uvw1$ colors of the three SC SNe Ia showed with respect to the shaded region of normal SN Ia colors. For comparison, SNe similar to SNe 1991T and 2002cx are also plotted. SC SNe Ia are distinctly bluer than the normal SNe Ia, but some of the 1991T-like and 2002cx-like SNe can be just as blue.

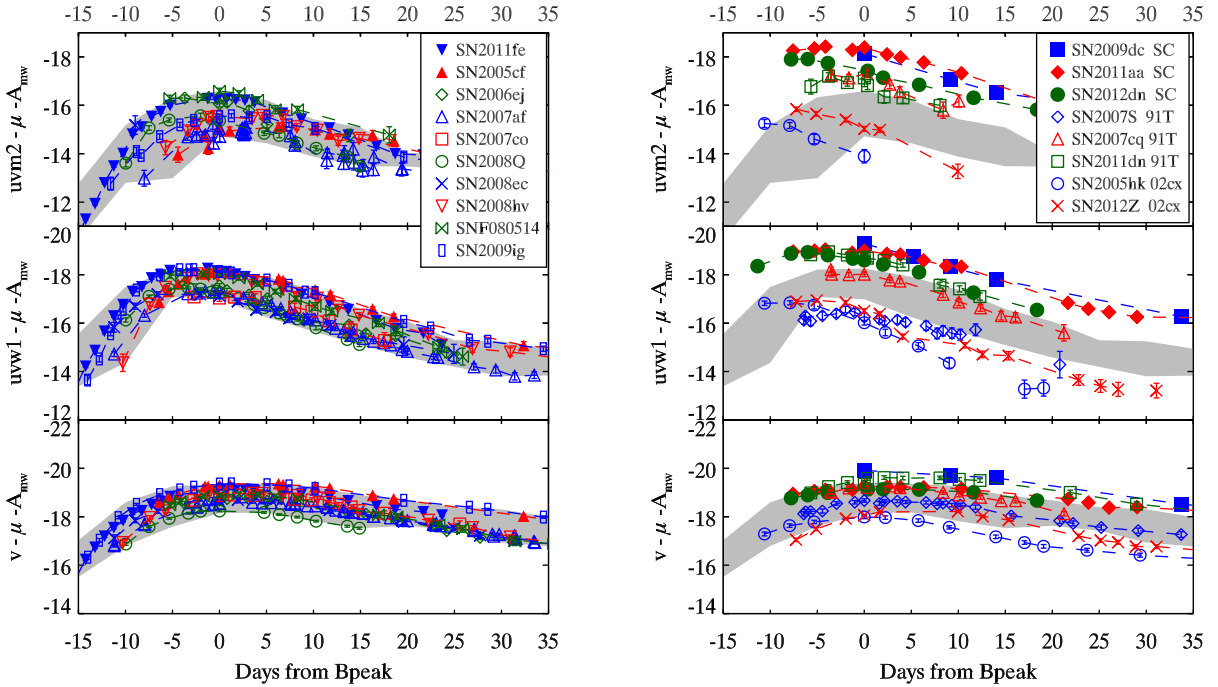


Figure 4. Left: Absolute magnitudes (correcting for distance modulus and MW extinction) of normal SNe Ia observed by Swift with shaded region showing their range. The SNe are labeled the same as in the left panel of Figure 3. The curves of individual SNe are not as important as the range of absolute magnitudes at various epochs. Right: Absolute magnitudes (correcting for distance modulus and MW extinction) of the three SC SNe Ia showed with respect to the shaded region of normal SN Ia absolute magnitudes. For comparison, SNe similar to SNe 1991T and 2002cx are also plotted. SC and 1991T-like SNe Ia are at the bright end of the normal distribution in the optical and distinctly brighter in the UV. The 2002cx-like SNe are at the faint end of the normal distribution in the optical but become relatively brighter (and peak much earlier) in the mid-UV.

before the optical maximum and then becoming redder again. The $uvm2-uvw1$ colors of SNe Ia have a large dispersion and tend to become slowly bluer. The range of normal SN colors is compared to our SC sample in the right panel. SN 2009dc, which was first observed near the optical maximum, is at the blue end of both colors but not extremely so. SN 2012dn has similar colors at similar epochs but was also observed at earlier epochs. At those pre-maximum epochs SN 2012dn was bluer than the normal SNe. SN 2011aa had similar premaximum colors to SN 2012dn but did not redden as quickly as the others due to the slower light curve evolution shown above.

Milne et al. (2013a) suggest that the spread in the NUV colors of normal SNe Ia can be viewed as two separate subclasses. In addition to their bluer colors, the NUV-blue subclass also shares a spectroscopic trait with SC SNe in showing CII in their optical spectra Thomas et al. (2011); Milne et al. (2013a). SNe 2003fg (Howell et al. 2006), 2006gz (Hicken et al. 2007), 2007if (Yuan et al. 2010; Scalzo et al. 2010), 2009dc (Taubenberger et al. 2011; Silverman et al. 2011), and 2012dn (Parrent & Howell 2012) all noted CII, often very strong. Two slow-decliners that aren't considered SC candidates, 2001ay and 2009ig, may have had weak CII features (Krisciunas et al. 2011; Foley et al. 2012b).

While SN 2009dc is actually included in the NUV-blue subclass (as the bluest member) in Milne et al. (2013a), the early phase observations of SNe 2011aa and 2012dn presented here show that the SC SNe are much bluer than normal SNe Ia at earlier times. SC SNe may not have the early red to blue evolution of normal SNe Ia, or it happens earlier than ten days before optical maximum. Their slower evolution, on the other hand, might make the time of optical maximum a poor reference point for giving physical meaning to their behavior compared to normal SNe Ia. Nevertheless, it is clear that the SC SNe Ia extend the diversity in the UV more than that already found (Brown et al. 2009; Wang et al. 2012; Milne et al. 2013a). Early UV observations appear to be a way of photometrically separating SC SNe from normal SNe. This could be quantified as the magnitude or timing of the minimum color (i.e. the color at its bluest epoch) or the time difference between maximum light in the UV and optical bands.

Two additional classes of SNe also warrant further comparison. Spectroscopic similarity to SN 1991T was used as a follow up criterion to discover new SC candidates by Scalzo et al. (2012). SNe similar to SN 2002cx (also called SNe Iax; Foley et al. 2013) also show hot, highly-ionized photospheres. We are not making a physical connection between the groups, but they warrant further comparison because of how their similar physical conditions have a strong effect on their UV flux and because of possible confusion in spectroscopic classification (Foley et al. 2013). Several examples of each are displayed in the right hand panel of Figure 3. Similar to the SC SNe, 1991T-like and 2002cx-like SNe showed a monotonic reddening in $uvw1-v$ from the onset of Swift observations. With the exception of SN 2007S (whose optical colors suggest reddening from the host galaxy; Brown et al. 2010), all could have been as blue (in $uvw1-v$) as the SC SNe if they were observed early enough but the colors became redder at a much faster rate than the SC SNe. In the $uvm2-uvw1$ color, one of each class had

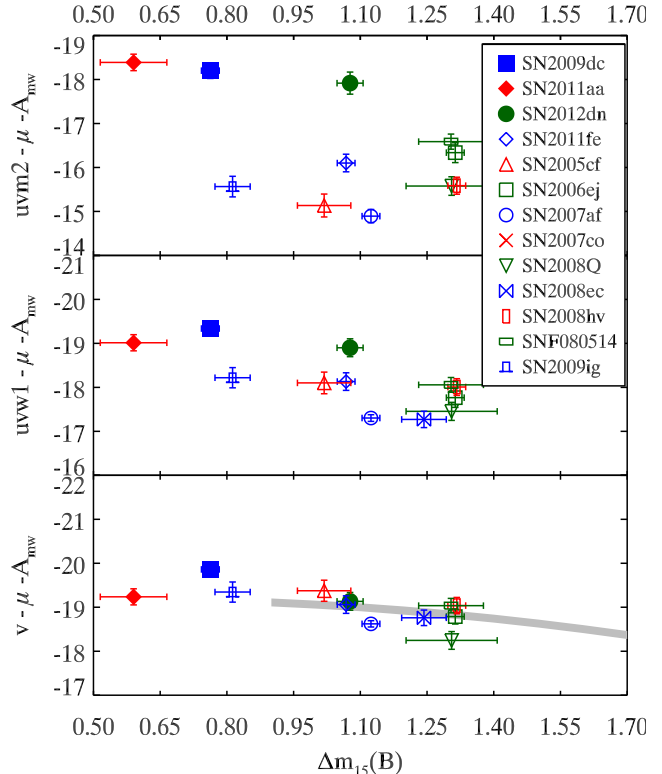


Figure 5. Peak Absolute magnitudes (correcting for distance modulus and MW extinction) of normal and candidate SC SNe Ia observed by Swift. The absolute magnitude v , $\Delta m_{15}(B)$ relation of Phillips et al. (1999) is plotted as a grey band with a width corresponding to the 1σ uncertainty. The Swift sample of normal SNe Ia is consistent with the relation but has a large scatter (due primarily in the optical to distance uncertainties; see Brown et al. 2010). Of the three SC SNe Ia observed by Swift, all three are overluminous in the UV but only SN 2009dc is overluminous in the optical. The y-axis is the same in all three panels to show how the scatter in absolute magnitudes increases to shorter wavelengths (Brown et al. 2010) as does the separation in brightness between the SC SNe and the normal SNe Ia.

a comparable color. The 91T-like SN 2007cq was classified by Milne et al. (2013a) as a MUV-blue, because it follows the NUV-red group in $uvw1-v$ but is relatively blue in $uvm2-uvw1$. Thus multi-epoch multi-wavelength UV photometry reveals complicated similarities and differences amongst SNe of different subclasses and within the same subclass. Further observations of members of these classes, including UV spectroscopy and even earlier UV photometry, will help explain the physical origins of the UV flux.

3.3. Absolute Magnitudes

Since one common characteristic of the strongest SC SN candidates is their high luminosity, we now examine the absolute magnitudes of SNe 2009dc, 2011aa, and 2012dn. As in Brown et al. (2010), most distance moduli are computed from the host galaxy recessional velocity, corrected for local velocity flows (Mould et al. 2000), and a Hubble constant of 72 km/s/Mpc (Freedman et al. 2001). Distances from Cepheids, the Tully-Fisher relation, or surface brightness fluctuations are used when available, as listed in Brown et al. (2010) and Brown et al. (2012b). For SNe 2009dc, 2011aa, and 2012dn the adopted Hubble flow distances are $34.94 \pm$

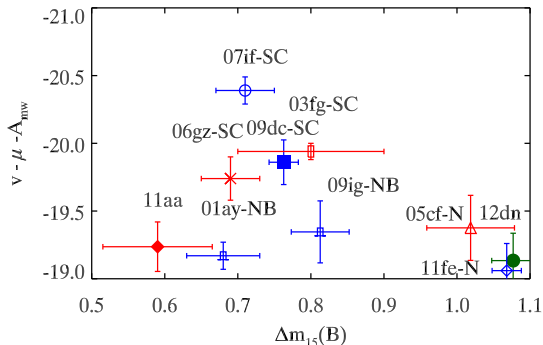


Figure 6. Peak Absolute magnitudes in the V band (correcting for distance modulus and MW extinction) of normal and candidate SC SNe Ia with $\Delta m_{15}(B) < 1.1$ observed by Swift with additional broad SNe observed from ground-based facilities. SN 2009dc has a comparable V-band brightness as the other probable Super Chandrasekhar-mass SNe (marked with ‘SC’). The two new SC SN candidates discussed here have optical absolute magnitudes comparable to the normal but broad (‘NB’) SNe 2001ay and 2009ig and the very normal SNe 2005cf and 2011fe (marked with a ‘N’).

0.16, 33.894 ± 0.18 , and 33.324 ± 0.20 , respectively. The SNe in this sample are at relatively low redshifts (mostly with recessional velocities less than 6000 km/s), so thermal velocities of the galaxies can add a significant dispersion to distances calculated assuming a Hubble flow. Thus the scatter of absolute magnitudes in the optical is much larger than found for larger samples of SNe (see Brown et al. 2010 for more details on this sample). Maeda et al. (2009) suggest that the extinction and thus the luminosity of SN 2006gz could be overestimated. To avoid such overcorrections, we do not correct any of the SNe Ia for host extinction. We do correct for line sight extinction in the Milky Way (MW) by converting the Schlafly & Finkbeiner (2011) V-band extinction from NED to an E(B-V) reddening (by dividing by 3.1) and then multiplying by the extinction coefficients calculated for the UV-optical spectrum of SN 1992A (Brown et al. 2010).

Figure 4 shows the absolute magnitudes in the optical (v band), NUV (uvw1), and MUV (uvm2). While SC SNe Ia are brighter than most (but not all; see below) in the optical, they are almost one magnitude brighter than the brightest in the NUV and about two magnitudes brighter in the MUV. The light curve shapes are similar in shape, but SN 2012dn fades a little faster while SNe 2009dc and 2011aa remain brighter than normal SNe Ia for a month after peak. For comparison, SNe similar to SNe 1991T and 2002cx are also plotted. SC and 1991T-like SNe Ia are at the bright end of the normal distribution in the optical and distinctly brighter in the UV. The 2002cx-like SNe are at the faint end of the normal distribution in the optical but become relatively brighter (and peak much earlier) at shorter wavelengths.

Figure 5 shows the peak absolute magnitudes compared to $\Delta m_{15}(B)$ for the normal and SC SNe Ia. The SC SNe candidates all have broad optical light curves (i.e. low values of $\Delta m_{15}(B)$) but not uniquely broad. In the UV, all three are noticeably brighter. The peak optical luminosities of SNe 2011aa and 2012dn are comparable to those of the normal SNe Ia. SN 2009dc is significantly brighter in the optical. Figure 6 zooms in on the absolute v-band magnitudes of the broad SNe, including ground

based observations of other broad SNe. SN 2009dc lies clearly amongst the other SC SNe while SNe 2011aa and 2012dn have v-band absolute magnitudes consistent with the other SNe Ia. The absolute magnitudes, especially in the UV, are very sensitive to the extinction. One concern for the analysis of SN 2006gz based on the luminosity is that it is very sensitive to the assumed extinction – SN 2006gz could be fainter if there is less host extinction or if the extinction coefficient is smaller. In multiple analyses SN 2009dc is bright even if no host galaxy extinction is assumed but could be even brighter. In this plot we have assumed no host dust extinction, yet they could be extinguished by dust in the host galaxy, and thus intrinsically brighter. The extremely blue colors would suggest that the host reddening is minimal, but the intrinsic colors of these objects are not actually known. A larger sample is needed to determine observationally what the range of colors might be and how blue the unreddened color could be. The degeneracy between reddening and luminosity means that the SNe 2011aa and 2012dn could have low reddening and be optically underluminous compared to SN 2009dc. Alternatively, significant reddening would mean they are intrinsically bluer and even more overluminous in the UV. Either way, these three SNe show similarities but are not identical.

3.4. Spectral Comparisons

Figure 7 shows the UVOT grism spectra of SNe 2009dc, 2011aa, and 2012dn. The signal to noise ratio is much lower than usual for optical SN spectroscopy, but comparable to other Swift/UVOT spectra (Bufano et al. 2009; Foley et al. 2012b). SN 2011aa was contaminated by an overlapping stellar spectrum, but SNe 2009dc and 2012dn exhibit similar continuum shapes and features. Absorption from MgII appears in the NUV, while shortward of that the spectrum is blanketed by overlapping lines of iron-peak elements. The bottom panel of Figure 7 compares the combined UVOT-SALT spectrum of SN2012dn to an HST UV/optical spectrum of SN 2011fe taken 2011 September 7 (2.9 days before maximum light in the B band; Mazzali et al. 2013) and a Swift/UVOT grism spectrum of the broad but normal SN 2009ig (Foley et al. 2012b) taken 2009 September 3.7 (2.3 days before maximum light in the B band). All three spectra have been normalized to the same b-band magnitude to compare the relative flux in the UV.

SN 2011fe, classified as a NUV-blue SN (Milne & Brown 2012; Milne et al. 2013a), and SN 1009ig are not dissimilar to SN 2012dn above 4000 Å. The CaII H&K lines of SN 2009ig are very broad and deep (Foley et al. 2012b; Marion et al. 2013), reducing its NUV flux. In the MUV, SNe 2009ig and 2011fe have a much lower flux and a smoother pseudo-continuum. While we do not want to overinterpret the grism spectrum by studying individual features at this time, the strong undulations in the MUV of SNe 2009dc and 2012dn suggest a lower opacity (and thus gaps in the line blanketing), rather than a hot blackbody from a shock interaction, as the source of the increased UV luminosity.

3.5. Integrated Luminosity

To determine how much flux is observed, we need to convert from the observed magnitudes. Flux conver-

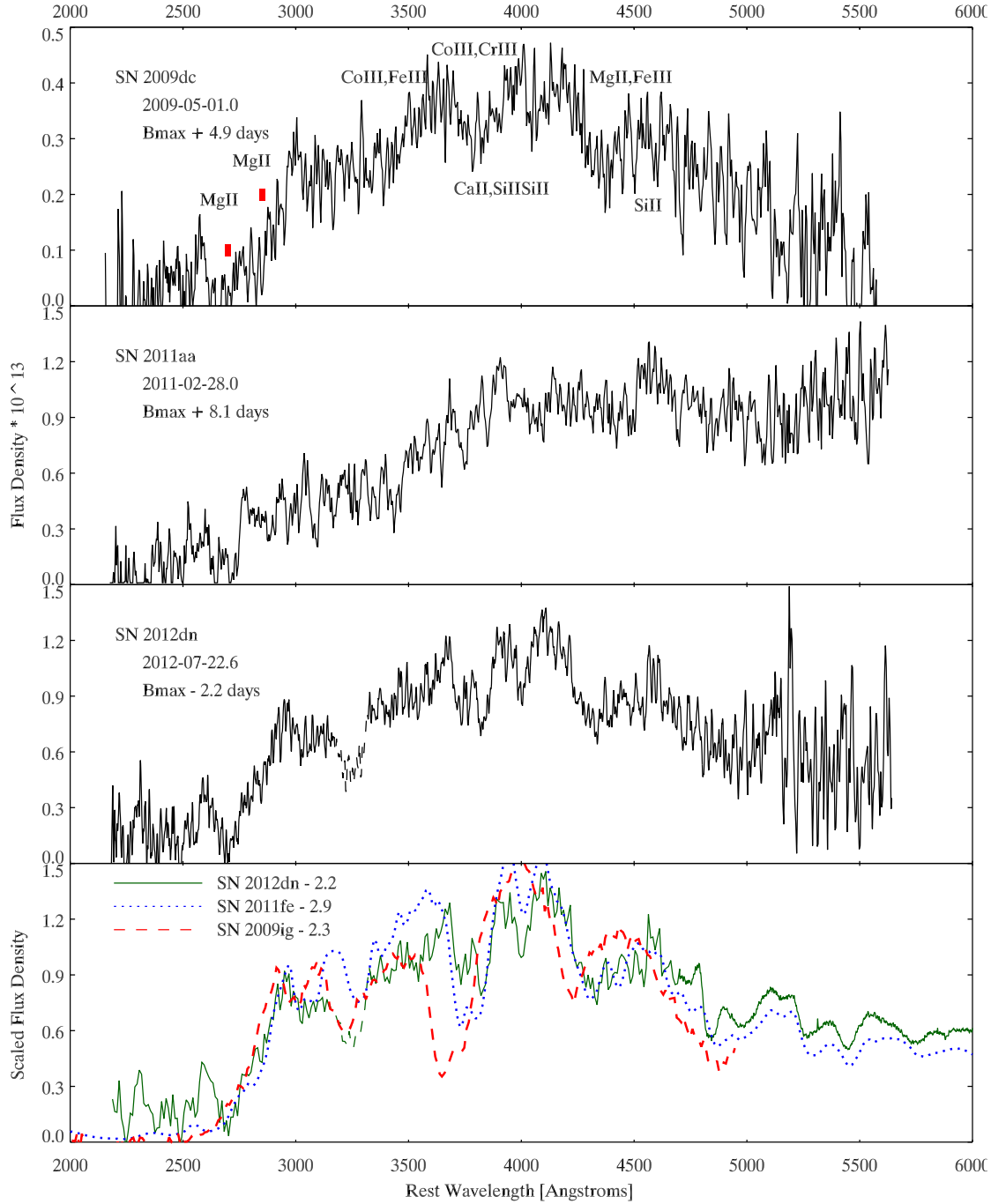


Figure 7. Top: UVOT grism spectrum of SN 2009dc. The position of NUV MgII lines are marked (for a velocity of 9000 km/s). The other line identifications are from Hachinger et al. (2012). Top Middle: UVOT grism spectrum of SN 2011aa. There is significant contamination from an overlapping stellar spectrum. This spectrum is shown here for completeness but not utilized further. Bottom Middle: UVOT grism spectrum of SN 2012dn. The absorption region between 3250 and 3400, set apart by a dashed line, is due to a readout streak from a bright source in the background region. Bottom: Combined spectrum of SN 2012dn compared to normal SNe Ia 2011fe and broad 2009ig. For comparison purposes, all spectra are normalized to have the same B band magnitude. The NUV continuum of SN 2012dn is not significantly different than the NUV-blue SN 2011fe, while SN 2009ig has broader absorption features. Shortward of 2700 Å, SN 2012dn has a clear MUV excess composed of strong features rather than the smooth continuum with diluted features expected if the excess luminosity were due to a hot blackbody spectrum from shock interaction.

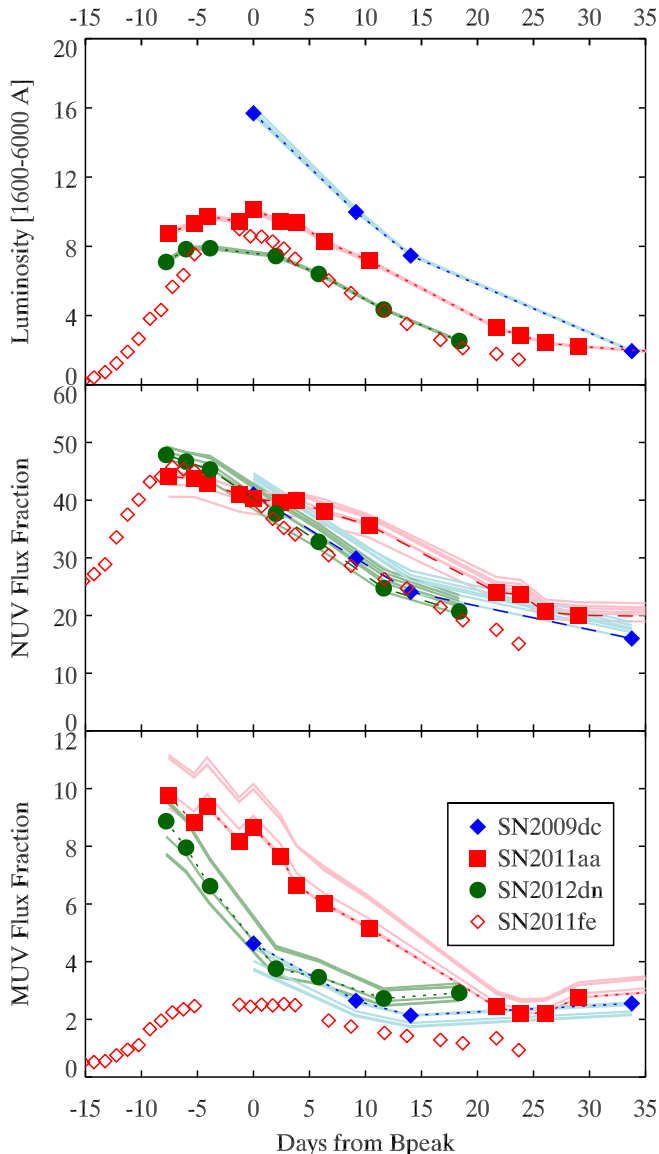


Figure 8. Top: Integrated flux from 1600 to 6000 Å. SN 2009dc is about twice as bright as SNe 2011aa and 2012dn which have about the same brightness as SN 2011fe. Faint lines in all three plots represent flux reconstructions using different spectral templates. The difference is negligible in the integrated luminosity so the lines overlap. Middle: Fractions of the 1600-6000 Å integrated flux in the NUV (2800 - 4000 Å) region for the SC SNe Ia compared to the NUV-blue normal SN 2011fe. The NUV fractions for normal SNe Ia peak between 30 (for NUV-red SNe Ia) and 40% (For NUV-blue) with the SC SNe Ia all near 40%. Bottom: Fractions of the 1600-6000 Å integrated flux in the MUV (1600 - 2800 Å) region for the SC SNe Ia compared to the NUV-blue normal SN 2011fe. SNe 2012dn and 2011aa have 10 and 9%, respectively, of their flux in the MUV in their earliest observation. By B-band maximum light, the fraction for SN 2012dn has dropped down to 4%, only modestly above SN 2011fe. SN 2011aa has a significantly larger fraction of its flux (compared to the others) for at least ten days after the B-band maximum.

sion factors are very spectrum dependent in the UV (Brown et al. 2010), differing by source type and phase for objects (like SNe) with time-variable spectra. Simpler SEDs based on the photometry have a problem reproducing the multi-filter photometry. To estimate the flux contributions of different wavelength regions, we use the

combined UV/optical spectrum we have for SN 2012dn and warp it to match the photometry as follows. First, the spectrum was smoothed with a running average over 10 Å. The spectrum is extrapolated beyond the UVOT filter range using the mean of the spectrum in the shortest 50 Å (between 2200 and 2250 Å). Then the whole spectrum was scaled by a constant value to match the observed b-band magnitude at that epoch. A warping function is created from linear segments from 1500 Å to 8100 Å (just beyond the UVOT bounds) with pivot points near where the UVOT filter curves intersect each other (after normalizing by the integral of the effective area of the curve to deweight the broader filters). These points are at 2030, 2460, 3050, 3870, and 4960 Å. These seven points are iteratively adjusted to minimize the magnitude differences between the observed photometry and that of the warped spectrum. This method better reproduces the spectral shape than converting the observed photometry to independent flux density points and simply connecting the dots (Brown et al. 2014, in preparation). The SN2012dn spectrum is used for SNe 2012dn and 2011aa. For SN 2009dc we combine the UVOT grism spectrum with a comparable epoch spectrum from Taubenberger et al. (2011) obtained from the WISEREP database⁷ (Yaron & Gal-Yam 2012).

From these warped spectra we calculate the amount of flux coming from the full UVOT range (1600 - 6000 Å) and three regions – MUV (1600 - 2800 Å), NUV (2800 - 4000 Å), and optical (4000 - 6000 Å) at each epoch with photometry in all six UVOT filters. The top panel of Figure 8 shows the integrated flux of the three SC SNe compared to a direct integration of the UV/optical spectra of Pereira et al. (2013) for the normal NUV-blue SN 2011fe. Despite their bright UV luminosity, SNe 2011aa and 2012dn which have about the same integrated luminosity as the normal SN 2011fe. SN 2009dc is about twice as bright. The evolution of the MUV and NUV flux fractions (compared to the total 1600 - 6000 Å flux) are displayed in the middle and lower panel of Figure 8. The NUV fractions for the SC SNe SN 2011fe all peak between 44 and 48%. SNe 2012dn and 2011aa have 10 and 9%, respectively, of their flux in the MUV in their earliest observation. By B-band maximum light, the fraction for SN 2012dn has dropped down to 4%, only modestly above SN 2011fe. SN 2011aa has a significantly larger fraction of its flux (compared to the others) for at least ten days after the B-band maximum. As a simple check on the effect of the template spectrum we perform the same color matching for all three SNe using the SNe 2009dc and 2012dn spectra, UV/optical spectra of SN 2011fe from Pereira et al. (2013) near maximum light and 24 days after maximum, the near maximum spectrum of the SN Ia 1992A from Kirshner et al. (1993) and a spectrum of Vega from Bohlin & Gilliland (2004). The total flux changes by only a few percent and the MUV fraction changes by up to 15% (in a relative sense), indicating that the luminosity measurement is dependent on, but not dominated by, the spectral template input.

The integrated luminosity curves allow us to compare in a relative sense the bolometric luminosity of SNe 2011aa and 2012dn to the well-studied SN 2009dc, and

⁷ <http://www.weizmann.ac.il/astrophysics/wiserep/>

thus the inferred ^{56}Ni mass. Since the colors of SNe 2011aa and 2012dn are similar to or bluer in color than SN 2009dc, we assume for now that they do not suffer significantly more dust extinction than SN 2009dc and that the same fractions of the bolometric luminosities lie outside of our 1600–6000 Å range for all three SNe. We also assume the rise time is similar for the three SNe and that the ratio of the bolometric luminosity to the radioactive luminosity is the same. Under these (many) assumptions, the mass of ^{56}Ni is proportional to the integrated luminosity $L_{1600-6000}$. For a range of host galaxy reddening values, Silverman et al. (2011) determined a ^{56}Ni between 1.2 and 3.7 M_{\odot} , with a most likely value of $1.7 \pm 0.4 M_{\odot}$. Since SNe 2011aa and 2012dn have about half the integrated luminosity, their ^{56}Ni would likely be around 0.9 M_{\odot} . While smaller than SN 2009dc, it is close to the amount of ^{56}Ni produced (0.92 M_{\odot}) in a Chandrasekhar-mass detonation where the entire mass is converted into iron group elements (Khokhlov et al. 1993). One could also make the comparison with SN 2011fe. Because of its smaller luminosity and shorter rise time (16.58 days for SN 2011fe compared to at least 21.1 days for SN 2009dc), the ^{56}Ni mass is estimated to be 0.53 M_{\odot} (Pereira et al. 2013). If SNe 2011aa and 2012dn were assumed to have similar rise times and radiative efficiencies as SN 2011fe, the ^{56}Ni masses would also be similar. So the estimate relies in part on assumptions about an unobserved property—the rise time. The observed properties of SNe 2011aa and 2012dn are more similar to SN 2009dc than SN 2011fe, but this highlights the need for a better understanding these objects and limiting the assumptions that must be made. Further analysis is needed to determine more accurately the ^{56}Ni mass required and what progenitor/explosion scenarios might result in these observables.

4. DISCUSSION AND SUMMARY

One suggestion for the increased luminosity in SC SNe is shock interaction (Fryer et al. 2010; Blinnikov & Sorokina 2010; Taubenberger et al. 2011; Hachinger et al. 2012). Scalzo et al. (2012) suggest UV observations as a means to probe the influence of shock interactions on the early luminosity. Fryer et al. (2010) performed numerical calculations of the spectra and simulated UVOT light curves resulting from a double-degenerate SN Ia exploding within a shell of unaccreted material. While our candidate SC SNe Ia have peak luminosities comparable to those studied by Fryer et al. (2010), the light curves shapes are much different. The light curve shapes can vary based on the amount and spatial distribution of the surrounding material, but the smoothness of the UV light curves and their qualitative similarity to the optical light curves suggest a photospheric origin.

A photospheric origin for the emission is supported by the UV spectra of SNe 2009dc and 2012dn, which show stronger features in the MUV (below 2700 Å) than seen in normal SNe Ia, while the flux from a hot shock would be relatively smooth and would dilute the photospheric features (Hamuy et al. 2003). On the other hand, the optical features are also much stronger than for SN 2007if, for which the top lighting of a shock was invoked as one explanation for its diluted features and high luminosity (Scalzo et al. 2010). The UV spectra of SNe 2009dc and

2012dn do not allow a smooth blackbody source for the excess flux. Such a spectrum might be expected from a high temperature shock with a hydrogen-rich circumstellar medium, as was used to explain the diluted features of SN 2002ic (Hamuy et al. 2003, see also Branch et al. 2000). A structured spectrum with emission and absorption, due to reprocessing of the shock emission or originating from a different composition, cannot be excluded. Hachinger et al. (2012) found adding a spectrum of the Ibn SN 2006jc to their theoretical SN Ia spectrum gave reasonable matches to the observed spectra of SN 2009dc. Higher quality UV spectra of Ibn and SC SNe are needed to perform similar tests in the UV. Nevertheless, photometric observations may already contain enough information to further constrain photometric (e.g. Kamiya et al. 2012) or spectroscopic modeling (e.g. Hachinger et al. 2012).

While the optical light curves of SNe 2011aa and 2012dn are not dissimilar to normal SNe Ia (though extremely broad in the case of SN 2011aa), the NUV-optical and especially the MUV-NUV (or MUV-optical) colors are markedly different. The rest-frame UV also peaks earlier for SC than normal SNe Ia. Early rest-frame UV photometry might allow optically overluminous SNe such as SN 2009dc to be excluded from cosmological analysis. Scalzo et al. (2012) estimate the rate of SC SNe to be a few percent of all SNe Ia locally, but a bias could result from an evolutionary shift (Taubenberger et al. 2011) if these are more common in the early universe than they are locally. Milne et al. (2013b) show that the relative fractions of NUV-blue and NUV-red normal SNe Ia change with redshift. The origin of the UV diversity amongst normal and SC candidate SNe Ia may point to ways to reduce the dispersion at longer wavelengths and understand potential biases in SN Ia standardization at different epochs in the history of the universe.

Bolometric light curve comparisons between models and observations serve as an important diagnostic of allowed models and parameters. The creation of bolometric light curves, however, especially the treatment of missing wavelength ranges, varies greatly. Sometimes the NUV (or at least the ground based U band) is included, and the MUV may or may not be included. Often the UV portion of the flux is considered to be negligible (a reasonable assumption in some cases). If it is included, it is often set at a constant percentage of the flux. As shown here, there is also a lot of variation in the NUV and MUV flux fractions between various SNe Ia, and the fractions evolve quite significantly with time.

The data given here will allow the bolometric light curves of these objects to be more accurately determined. For example, the falling UV fraction means that inclusion of the UV flux will broaden the pre-maximum rise of the bolometric flux. This could lead to a longer implied rise time if fit with a light curve template. This longer rise time may not be accurate, however, if the stretched light curve template did not include the UV in its construction. Kamiya et al. (2012) use multi-wavelength modeling to show the difference between a BVRI, UV-Optical-IR (UVOIR), and true bolometric light curve. The distinction between these is important. UV data will allow more constraints on the modelling.

While we have pushed the knowledge of the UV be-

havior for SC SNe Ia ~ 8 days earlier, the very earliest epochs would also be important for looking for the effects of shock interaction with a non-degenerate companion (Kasen 2010; Brown et al. 2012a) or differences in the UV-optical flux evolution at the earliest times (Brown et al. 2012b). As the UV-optical colors are still bluest at the first epochs observed, the bolometric contribution before then may be larger still and are in any case uncertain. Higher quality UV spectra at the earliest possible epochs will better probe the mechanism responsible for the excess UV emission and how to account for it in mass determinations.

In summary, we have presented UV/optical photometry and spectroscopy for three SNe Ia, 2009dc, 2011aa and 2012dn, which have been suggested as candidate super-Chandrasekhar mass SNe Ia. While their optical properties are not dissimilar to normal SNe Ia, they are significantly bluer and more luminous in the UV than normal SNe Ia, with MUV luminosities about a factor of ~ 10 higher. UV spectra of SNe 2009dc and 2012dn feature structure not expected for shock interaction, suggesting a photospheric origin of the excess UV luminosity. The UV is shown to contribute significantly (but still smaller than the optical) to the bolometric luminosity, especially at early times. The integrated luminosities of SNe 2011aa and 2012dn are much lower than 2009dc, however. This suggests a larger diversity in the class, if they are indeed in the same class, when considering UV and optical photometric and spectroscopic characteristics. A more detailed study of these SNe is required to determine if they were above the Chandrasekhar mass.

P.J.B. is supported by the Mitchell Postdoctoral Fellowship and NSF grant AST-0708873. P.A.M. acknowledges support from NASA ADAP grant NNX10AD58G. We are grateful to J. Vinko and J. Parrent for sharing the spectra of SN 2012dn. We are also grateful to H. Marion and X. Wang for looking at optical spectra of SN 2011aa. This work made use of public data in the *Swift* data archive and the NASA/IPAC Extragalactic Database (NED), which is operated by the Jet Propulsion Laboratory, California Institute of Technology, under contract with NASA.

REFERENCES

- Arnett, W. D. 1982, *ApJ*, 253, 785
- Bianco, F. B., Howell, D. A., Sullivan, M., et al. 2011, *ApJ*, 741, 20
- Blinnikov, S. I., & Sorokina, E. I. 2010, *ArXiv e-prints*
- Bloom, J. S., Kasen, D., Shen, K. J., et al. 2012, *ApJ*, 744, L17
- Bock, G., Parrent, J. T., & Howell, D. A. 2012, *Central Bureau Electronic Telegrams*, 3174, 1
- Bohlin, R. C., & Gilliland, R. L. 2004, *AJ*, 127, 3508
- Branch, D. 1992, *ApJ*, 392, 35
- Branch, D., Jeffery, D. J., Blaylock, M., & Hatano, K. 2000, *PASP*, 112, 217
- Breeveld, A. A., Landsman, W., Holland, S. T., et al. 2011, in *American Institute of Physics Conference Series*, Vol. 1358, American Institute of Physics Conference Series, ed. J. E. McEnery, J. L. Racusin, & N. Gehrels, 373–376
- Brown, P. J., Dawson, K. S., Harris, D. W., et al. 2012a, *ApJ*, 749, 18
- Brown, P. J., Holland, S. T., Immler, S., et al. 2009, *AJ*, 137, 4517
- Brown, P. J., Roming, P. W. A., Milne, P., et al. 2010, *ApJ*, 721, 1608
- Brown, P. J., Dawson, K. S., de Pasquale, M., et al. 2012b, *ApJ*, 753, 22
- Bufano, F., Immler, S., Turatto, M., et al. 2009, *ApJ*, 700, 1456
- Copin, Y., Gangler, E., Pereira, R., et al. 2012, *The Astronomer's Telegram*, 4253, 1
- de Vaucouleurs, G., de Vaucouleurs, A., Corwin, Jr., H. G., et al. 1991, *Third Reference Catalogue of Bright Galaxies. Volume I: Explanations and references. Volume II: Data for galaxies between 0^h and 12^h. Volume III: Data for galaxies between 12^h and 24^h.*
- Dilday, B., Howell, D. A., Cenko, S. B., et al. 2012, *Science*, 337, 942
- Falco, E. E., Kurtz, M. J., Geller, M. J., et al. 1999, *PASP*, 111, 438
- Fink, M., Röpke, F. K., Hillebrandt, W., et al. 2010, *A&A*, 514, A53
- Foley, R. J., Simon, J. D., Burns, C. R., et al. 2012a, *ArXiv e-prints*
- Foley, R. J., Challis, P. J., Filippenko, A. V., et al. 2012b, *ApJ*, 744, 38
- Foley, R. J., Challis, P. J., Chornock, R., et al. 2013, *ApJ*, 767, 57
- Freedman, W. L., Madore, B. F., Gibson, B. K., et al. 2001, *ApJ*, 553, 47
- Fryer, C. L., Ruiter, A. J., Belczynski, K., et al. 2010, *ApJ*, 725, 296
- Ganeshalingam, M., Li, W., & Filippenko, A. V. 2011, *MNRAS*, 416, 2607
- Gehrels, N., Chincarini, G., Giommi, P., et al. 2004, *ApJ*, 611, 1005
- Goldhaber, G., Groom, D. E., Kim, A., et al. 2001, *ApJ*, 558, 359
- Gurugubelli, K., Sahu, D. K., Anupama, G. C., Anto, P., & Arora, S. 2011, *Central Bureau Electronic Telegrams*, 2653, 3
- Hachinger, S., Mazzali, P. A., Taubenberger, S., et al. 2012, *ArXiv e-prints*
- Hamuy, M., Phillips, M. M., Suntzeff, N. B., et al. 2003, *Nature*, 424, 651
- Hayden, B. T., Garnavich, P. M., Kasen, D., et al. 2010, *ApJ*, 722, 1691
- Hicken, M., Garnavich, P. M., Prieto, J. L., et al. 2007, *ApJL*, 669, L17
- Hillebrandt, W., Sim, S. A., & Röpke, F. K. 2007, *A&A*, 465, L17
- Horesh, A., Kulkarni, S. R., Fox, D. B., et al. 2012, *ApJ*, 746, 21
- Howell, D. A., Sullivan, M., Nugent, P. E., et al. 2006, *Nature*, 443, 308
- Iben, Jr., I., & Tutukov, A. V. 1984, *ApJS*, 54, 335
- Immler, S., Brown, P. J., Milne, P., et al. 2006, *ApJL*, 648, L119
- Jha, S., Riess, A. G., & Kirshner, R. P. 2007, *ApJ*, 659, 122
- Kamiya, Y. 2012, *Light Curve Model for SN 2011aa*, poster presented at *Supernovae Illuminating the Universe: from Individuals to Populations*, September 10–14, Garching bei Muenchen, Germany
- Kamiya, Y., Tanaka, M., Nomoto, K., et al. 2012, *ApJ*, 756, 191
- Kasen, D. 2010, *ApJ*, 708, 1025
- Khan, R., Stanek, K. Z., Stoll, R., & Prieto, J. L. 2011, *ApJ*, 737, L24
- Khokhlov, A., Mueller, E., & Hoefflich, P. 1993, *A&A*, 270, 223
- Kirshner, R. P., Jeffery, D. J., Leibundgut, B., et al. 1993, *ApJ*, 415, 589
- Krisciunas, K., Li, W., Matheson, T., et al. 2011, *AJ*, 142, 74
- Kromer, M., Sim, S. A., Fink, M., et al. 2010, *ApJ*, 719, 1067
- Kudelina, I., Gorbovskoy, E., Balanutsa, P., et al. 2011, *The Astronomer's Telegram*, 3164, 1
- Li, W., Bloom, J. S., Podsiadlowski, P., et al. 2011, *Nature*, 480, 348
- Maeda, K., & Iwamoto, K. 2009, *MNRAS*, 394, 239
- Maeda, K., Kawabata, K., Li, W., et al. 2009, *ApJ*, 690, 1745
- Maguire, K., Sullivan, M., Patat, F., et al. 2013, *MNRAS*, 436, 222
- Margutti, R., Soderberg, A. M., Chomiuk, L., et al. 2012, *ApJ*, 751, 134
- Marion, G. H., Vinko, J., Wheeler, J. C., et al. 2013, *ApJ*, 777, 40
- Marion, H., Garnavich, P., Challis, P., Calkins, M., & Peters, W. 2009, *Central Bureau Electronic Telegrams*, 1776, 1
- Mazzali, P., Sullivan, M., Hachinger, S., et al. 2013, *ArXiv e-prints*
- Mazzali, P. A., Chugai, N., Turatto, M., et al. 1997, *MNRAS*, 284, 151

- Milne, P. A., & Brown, P. J. 2012, ArXiv e-prints
- Milne, P. A., Brown, P. J., Roming, P. W. A., Bufano, F., & Gehrels, N. 2013a, *ApJ*, 779, 23
- Milne, P. A., Foley, R., & Brown, P. J. 2013b, *ApJ* submitted
- Milne, P. A., Brown, P. J., Roming, P. W. A., et al. 2010, *ApJ*, 721, 1627
- Mould, J. R., Huchra, J. P., Freedman, W. L., et al. 2000, *ApJ*, 529, 786
- Nugent, P. E., Sullivan, M., Cenko, S. B., et al. 2011, *Nature*, 480, 344
- Parrent, J. T., & Howell, D. A. 2012, Central Bureau Electronic Telegrams, 3174, 2
- Patat, F., Chandra, P., Chevalier, R., et al. 2007, *Science*, 317, 924
- Pereira, R., Thomas, R. C., Aldering, G., et al. 2013, *A&A*, 554, A27
- Perlmutter, S., Aldering, G., Goldhaber, G., et al. 1999, *ApJ*, 517, 565
- Phillips, M. M., Lira, P., Suntzeff, N. B., et al. 1999, *AJ*, 118, 1766
- Poole, T. S., Breeveld, A. A., Page, M. J., et al. 2008, *MNRAS*, 383, 627
- Puckett, T., Moore, R., Newton, J., & Orff, T. 2009, Central Bureau Electronic Telegrams, 1762, 1
- Puckett, T., Newton, J., Balam, D. D., et al. 2011, Central Bureau Electronic Telegrams, 2653, 1
- Riess, A. G., Press, W. H., & Kirshner, R. P. 1996, *ApJ*, 473, 88
- Riess, A. G., Filippenko, A. V., Challis, P., et al. 1998, *AJ*, 116, 1009
- Roming, P. W. A., Kennedy, T. E., Mason, K. O., et al. 2005, *Space Science Reviews*, 120, 95
- Russell, B. R., & Immler, S. 2012, *ApJ*, 748, L29
- Scalzo, R., Aldering, G., Antilogus, P., et al. 2012, *ApJ*, 757, 12
- Scalzo, R. A., Aldering, G., Antilogus, P., et al. 2010, *ApJ*, 713, 1073
- Schaefer, B. E., & Pagnotta, A. 2012, *Nature*, 481, 164
- Schlafly, E. F., & Finkbeiner, D. P. 2011, *ApJ*, 737, 103
- Silverman, J. M., Ganeshalingam, M., Li, W., et al. 2011, *MNRAS*, 410, 585
- Simon, J. D., Gal-Yam, A., Gnat, O., et al. 2009, *ApJ*, 702, 1157
- Sternberg, A., Gal-Yam, A., Simon, J. D., et al. 2011, *Science*, 333, 856
- Tanaka, M., Kawabata, K. S., Yamanaka, M., et al. 2010, *ApJ*, 714, 1209
- Taubenberger, S., Benetti, S., Childress, M., et al. 2011, *MNRAS*, 412, 2735
- Taubenberger, S., Kromer, M., Hachinger, S., et al. 2013, *MNRAS*, 432, 3117
- Theureau, G., Bottinelli, L., Coudreau-Durand, N., et al. 1998, *A&AS*, 130, 333
- Thomas, R. C., Aldering, G., Antilogus, P., et al. 2011, *ApJ*, 743, 27
- Wang, X., Wang, L., Filippenko, A. V., et al. 2012, *ApJ*, 749, 126
- Webbink, R. F. 1984, *ApJ*, 277, 355
- Whelan, J., & Iben, Jr., I. 1973, *ApJ*, 186, 1007
- Woosley, S. E., & Kasen, D. 2011, *ApJ*, 734, 38
- Woosley, S. E., & Weaver, T. A. 1994, *ApJ*, 423, 371
- Yamanaka, M., Kawabata, K. S., Kinugasa, K., et al. 2009, *ApJ*, 707, L118
- Yaron, O., & Gal-Yam, A. 2012, *PASP*, 124, 668
- Yuan, F., Quimby, R. M., Wheeler, J. C., et al. 2010, *ApJ*, 715, 1338